JACS
JOURNAL OF THE AMERICAN CHEMICAL SOCIETY
pubs.acs.org/JACS
Article

High-Connectivity Triazolate-Based Metal–Organic Framework for Water Harvesting

Karla Ravin, Patrick Sarver, Bhavish Dinakar, Lukáš Palatinus, Peter Müller, Julius Oppenheim,* and Mircea Dincă*

Cite This: https://doi.org/10.1021/jacs.5c01062
Read Online
ACCESS | Metrics & More | Article Recommendations | Supporting Information

ABSTRACT: Increasing the connectivity of structural units presents a potentially valuable approach to improve hydrolytic stability in metal–organic frameworks (MOFs). We herein leverage this strategy by synthesizing the first tritopic benzotriazolate MOF, $Zn_5(OAc)_4(TBTT)_2$ (H_3TBTT = 2,4,6-tris(1*H*-benzo[*d*][1,2,3]triazol-5-yl)-1,3,5-triazine), which exhibits open metal sites, high connectivity, high porosity, and significant water uptake capacity. The MOF adopts a previously unknown topology with (3,6,6)-connectivity, which is supported by single-crystal electron diffraction and elemental analysis. The framework undergoes postsynthetic metal and anion exchange with $NiCl_2$, which increases the accessible pore volume and the net hydrophilicity of the framework. With this exchange, the apparent BET surface area increases from 1994 to 3034 m^2/g, and the water uptake step shifts from 56 to 33% relative humidity (RH). The high gravimetric capacity of the Ni-rich MOF, 0.98 g/g, translates to a working capacity of 0.64 g/g during a pressure swing cycle between 20 and 40% RH at 25 °C. Combining this performance with a less than 2% loss in working capacity over 100 cycles, the new material rivals the best MOF water sorbents to date.

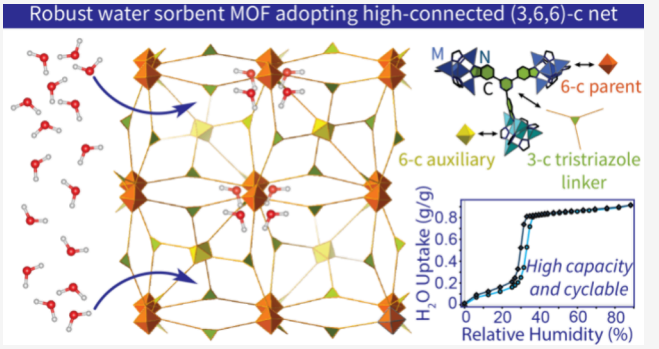

INTRODUCTION

Although the usage of metal–organic frameworks (MOFs) for water sorption applications such as atmospheric water harvesting has been well established,[1−4] the structure–function relationships that dictate hydrolytic and water cycling stability are still not fully understood. Empirically, it has been observed that early metal carboxylate MOFs (e.g., zirconium-carboxylate) or late-metal azolate MOFs (e.g., nickel-azolate) have superior kinetic stability toward water.[5] Among these, frameworks made from ditopic benzotriazolate ligands and late transition metals are particularly attractive for water sorption applications.[6−12]

Reasoning that the combination of multitopic ligands with highly connected secondary building units (SBUs) would further improve hydrolytic stability due to the entropic penalty for dissociation,[13,14] we sought to develop and study materials from multitopic triazolate linkers. Indeed, to our knowledge, there are no known examples of MOFs bearing benzotriazolate linkers having higher than ditopic connectivity. Herein, we report a new MOF, $Zn_5(OAc)_4(TBTT)_2$ ($TBTT^{3-}$ = 2,4,6-tris(1*H*-benzo[*d*][1,2,3]triazol-5-yl)-1,3,5-triazine), that exhibits both high connectivity (via tritopic linker and six-connected SBU) and kinetically inert late transition metal–benzotriazolate linkages (Figure 1). This framework adopts a novel (3,6,6)-c net. This topology is structurally analogous to the cubic **pcu** 6-c net of the well-known MFU-4*l*, but presents auxiliary connected pentanuclear Kuratowski clusters within the pores.[15] The framework is susceptible toward postsynthetic metal and anion exchange with $NiCl_2$ to yield a Ni-rich material with higher porosity, increased water capacity, and a lower RH water-uptake step, analogous to that demonstrated for CFA-1, which bears identical SBUs.[6] The Ni-exchanged framework is hydrolytically stable, demonstrating minimal degradation over 100 water cycles, and has a working capacity comparable to the top performing MOF water sorbents.

RESULTS AND DISCUSSION

Microcrystalline $Zn_5(OAc)_4(TBTT)_2$ was synthesized by solvothermal reaction between H_3TBTT and $Zn(OAc)_2$ in *N*,*N*-dimethylformamide (Supplemental Sections 2, 3, 9, and 10). The MOF crystallites were structurally characterized by electron diffraction (ED) as well as powder X-ray diffraction (PXRD). The electron diffraction reveals a framework obeying

Received: January 18, 2025
Revised: March 9, 2025
Accepted: March 11, 2025

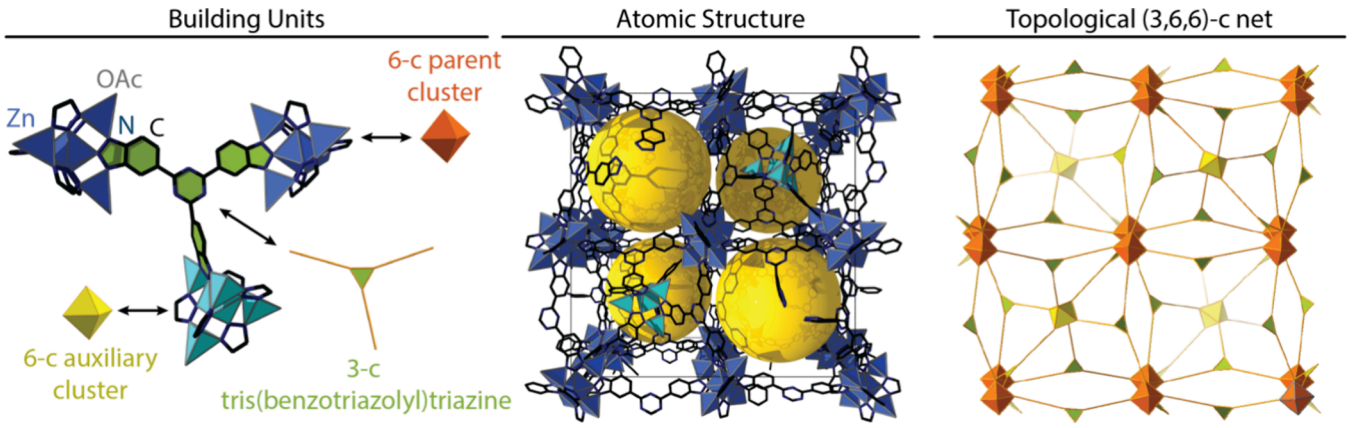

Figure 1. Model structure of $Zn_5(OAc)_4(TBTT)_2$ and its underlying (3,6,6)-connected net (shown in its augmented form) depicting the assembly from the three-connected tris(benzotriazolyl)triazine linker and 6-connected Kuratowski-cluster SBU. The SBUs depicted in blue and cyan are crystallographically distinct.

F-centering. Structure refinement in the space group $Fm\bar{3}m$ reveals a parent cubic framework with $Zn_5(OAc)_4(BTa)_6$ nodes (BTa = benzotriazole). The benzotriazole arms are connected via a triazine ring, which is disordered between edge-connected cubic pores. The third benzotriazole group on the triazine ring points into the cubic pore, forming an additional auxiliary SBU that occupies every other pore, resulting in disordered SBUs in this space group. The composition that allows for each and every dangling benzotriazolate to be coordinated to a $Zn_5(OAc)_4$-cluster is the MOF formula $Zn_5(OAc)_4(TBTT)_2$, which is supported by all elemental analyses: CHN combustion, Zn determination by inductively coupled plasma optical emissions spectrometry (ICP-OES), and Zn determination by thermogravimetric combustion to ZnO (Supplemental Sections 3 and 11).

Topological analysis of this structure reveals that there is a single possible tiling that enables full coordination, which can be represented as a (3,6,6)-c net in the space group $Pa\bar{3}$ where the $TBTT^{3-}$ linker is 3-connected, the SBU is 6-connected, and the auxiliary cluster is also 6-connected (Figure 1). This net can be derived from **xbk** (a 4,6,12-c net in $Fm\bar{3}m$), where half of the 12-connected nodes are eliminated or from **pcu** (a 6-c connected net in $Pm\text{-}3m$), where auxiliary nodes are added to half of the cubic pores (Figure S8.1). The symmetry of the idealized structure would descend from $Pa\bar{3}$ to $R3$, due to the presence of the noncentrosymmetric Kuratowski SBUs.

Given that no violations of F-centering systematic absences are observed, there must be a substantial number of defects within the structure, enabling a description as a disordered F-centered lattice. These defects are presumably missing auxiliary clusters, which leave dangling benzotriazole units pointed into the pores (potentially capped by zinc acetate moieties). Each local $R3$ domain of the idealized structure may be oriented with respect to each other by disorder by an inversion center, a mirror plane, or a 4-fold rotation, increasing the global symmetry to the observed $Fm\bar{3}m$.

As such, we present two different structural models. First, a refinement of the ED data in $Fm\bar{3}m$ with $a = b = c = 35.4$ Å. Here the parent cluster ($Zn_5(C_6N_3)_6$) and the triazine are well found in the electron density. However, the auxiliary Zn cluster and any dangling benzotriazole moieties are completely disordered in the pore and not included in the model. Second, a force field-optimized model structure of the idealized (3,6,6)-c topology (Figure 1). The only symmetry preserved by the topology and the geometry of the auxiliary cluster is a 3-fold rotation axis along the (111)-vector, implying $R3$. The primitive cell is a rhombohedral cell with dimensions $a = b = c = 35.4$ Å and $\alpha = \beta = \gamma = 90°$. This idealized cluster does not obey the systematic absences as noted by the F-centering (Figures 2, S4.3, and S4.4). Disagreement of the intensity for low resolution reflections between the simulated PXRD

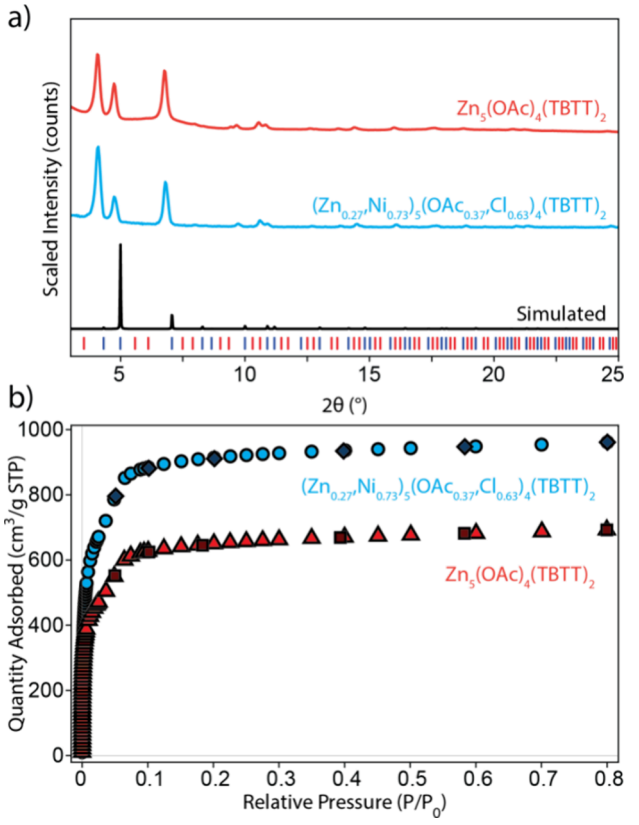

Figure 2. (a) PXRD patterns (Cu Kα) of $Zn_5(OAc)_4(TBTT)_2$ and $(Zn_{0.27},Ni_{0.73})_5(OAc_{0.37},Cl_{0.63})_4(TBTT)_2$ compared with the simulated ED $Fm\bar{3}m$ pattern (blue ticks), with additional marked angles (red ticks) corresponding to the $R3$ model. (b) 77 K nitrogen isotherms of each (after 170 °C activation) (adsorption depicted by triangle and circle markers and desorption depicted by square and diamond markers).

https://doi.org/10.1021/jacs.5c01062
J. Am. Chem. Soc. XXXX, XXX, XXX−XXX

Scheme 1. Postsynthetic Metal and Anion Exchange of $Zn_5(OAc)_4(TBTT)_2$ with $NiCl_2$

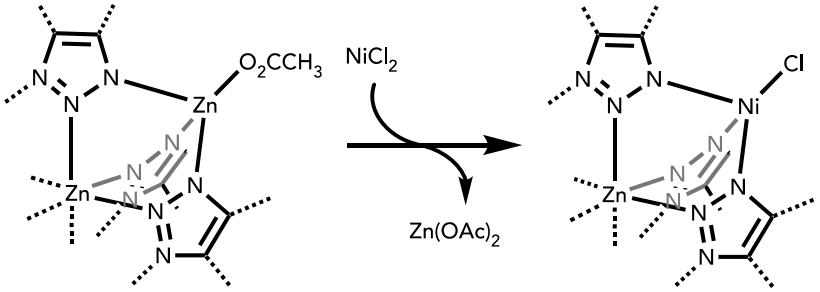

pattern from the $Fm\bar{3}m$ model and the experimental is attributed to the omission of the auxiliary cluster from the model and to disordered pore solvent. The simulated PXRD pattern of the *R*3 model, which contains an auxiliary cluster, (Figure S4.3) correctly reproduces the ratio of {111} to {200} reflection intensities.

Noting the improved kinetic stability typically imparted by Ni^{2+} ions, $Zn_5(OAc)_4(TBTT)_2$ was subjected to postsynthetic metal exchange with $NiCl_2$ mimicking established procedures (Scheme 1).[6] The PXRD patterns of the Ni-rich MOF are similar to the parent $Zn_5(OAc)_4(TBTT)_2$ with no significant loss in crystallinity or appearance of a secondary phase (Figure 2a). Inductively coupled plasma mass spectrometry (ICP-MS), energy-dispersive X-ray spectroscopy (EDS), and thermogravimetric combustion to the metal oxides were used to determine the Zn to Ni ratio as well as the acetate to chloride ratio, yielding the formula of a maximally substituted material $(Zn_{0.27},Ni_{0.73})_5(OAc_{0.37},Cl_{0.63})_4(TBTT)_2$ (Supplemental Sections 3 and 11).

Nitrogen adsorption isotherms at 77 K reveal apparent Brunauer–Emmett–Teller (BET) surface areas of 2088 ± 11 and 3034 ± 17 m^2/g and pore volumes of 1.07 and 1.49 cm^3/g for $Zn_5(OAc)_4(TBTT)_2$ and $(Zn_{0.27},Ni_{0.73})_5(OAc_{0.37},Cl_{0.63})_4(TBTT)_2$, respectively (Figure 2b, Supplemental Section 5). We attribute the diminished surface area of the parent MOF to the steric bulk of acetate anions as well as the disordered, dangling ligands within the pores from defects. Based on the chloride-capped structural model, the expected surface area is 3028 m^2/g and accessible pore volume is 1.35 cm^3/g, similar to that for the Ni-rich framework.

Water sorption measurements reveal high capacities for both $Zn_5(OAc)_4(TBTT)_2$ and $(Zn_{0.27},Ni_{0.73})_5(OAc_{0.37},Cl_{0.63})_4(TBTT)_2$. At 25 °C, the maximum gravimetric water uptake is 0.82 g H_2O/g MOF for the parent Zn MOF, and 0.98 g H_2O/g MOF for the Ni-rich framework. The maximum capacity decreases to 0.72 and 0.91 g/g after the third water cycle for the Zn-rich and Ni-rich materials, respectively (Figure 3, Supplemental Section 6). The critical relative humidity (RH), defined by the RH of the inflection point, occurs at 56% RH for the Zn-rich framework and shifts to 33% RH after exchange with Ni. The sharp uptake in adsorbed water, following a shallow uptake at low RH, is consistent with a capillary condensation mechanism preceded by prewetting on strongly interacting sites (such as the open metal sites and triazine nitrogens). After cycling, both MOFs retain their crystallinity (Figures S4.1 and S4.2).

The Ni-rich MOF's water sorption was measured at variable temperature (15, 25, and 35 °C) and the isosteric enthalpy was calculated to be 48 kJ/mol at the capillary condensation event,

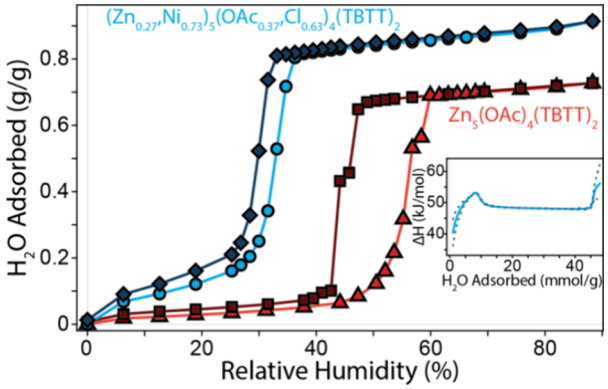

Figure 3. Isotherm for the adsorption of water vapor for the Zn and Ni-rich MOFs, as measured by the third cycle (adsorption depicted by triangle and circle markers and desorption depicted by square and diamond markers). Inset: The isosteric enthalpy of adsorption, ΔH, for the Ni-rich material.

indicating slightly stronger binding than that for bulk water at 44 kJ/mol (Figure S6.3).

In order to demonstrate the cycling stability of the Ni-rich MOF, we performed 100 adsorption–desorption cycles at 25 °C between 20 and 40% RH with 1 h equilibration periods for each half cycle (Figure 4). The RH range was chosen such that

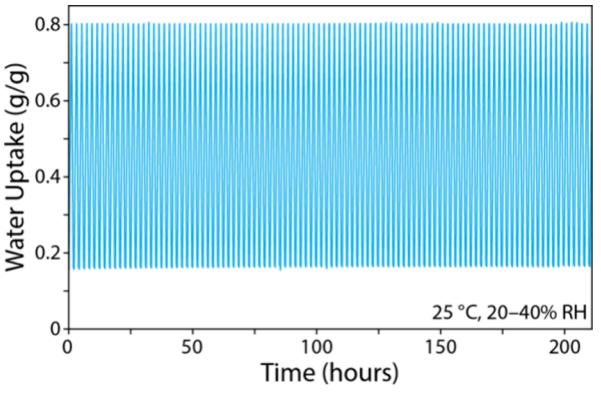

Figure 4. Pressure swing adsorption–desorption water cycling at 25 °C between 20 and 40% RH with 1 h adsorption and 1 h desorption cycles for $(Zn_{0.27},Ni_{0.73})_5(OAc_{0.37},Cl_{0.63})_4(TBTT)_2$.

the cycling would encompass the entire sharp sorption event. Over the course of this experiment, the working capacity decreased less than 2%, a performance comparable to that of Ni-CFA-1, one of the more stable, high-capacity MOFs for water sorption.[16,17] After cycling, the material retains crystallinity (Figure S4.2), consistent with our hypothesis

https://doi.org/10.1021/jacs.5c01062
J. Am. Chem. Soc. XXXX, XXX, XXX–XXX

that a high connectivity, Ni-triazolate MOF should show excellent hydrolytic stability.

CONCLUSIONS

The foregoing results report the first example of a tritopic benzotriazolate MOF, which indeed shows a novel topology, with a (3,6,6)-c net. Post synthetic metal exchange of the parent framework $Zn_5(OAc)_4(TBTT)_2$ with nickel yields $(Zn_{0.27},Ni_{0.73})_5(OAc_{0.37},Cl_{0.63})_4(TBTT)_2$, which exhibits high water cycling stability, which we assign to a combination of high kinetic stability of the Ni-benzotriazolate bonds, as well as high connectivity in both ligand and SBU. These new materials, which contain a high density of Kuratowski clusters, provide a complement to other MOFs bearing the same or similar clusters.[11,15,18−21]

ASSOCIATED CONTENT

Supporting Information

The Supporting Information is available free of charge at https://pubs.acs.org/doi/10.1021/jacs.5c01062.

General information, synthetic procedures, elemental analysis, PXRD patterns, nitrogen isotherms, water isotherms, scanning electron microscopy, crystallographic information, nuclear magnetic resonance spectroscopy, infrared spectroscopy, thermogravimetric analysis, model structure, and crystallographic information on $Zn_5(OAc)_4(TBTT)_2$ (PDF)

Accession Codes

Deposition number 2400065 contains the supplementary crystallographic data for this paper. These data can be obtained free of charge via the joint Cambridge Crystallographic Data Centre (CCDC) and Fachinformationszentrum Karlsruhe Access Structures service.

AUTHOR INFORMATION

Corresponding Authors

Julius Oppenheim − *Department of Chemistry, Massachusetts Institute of Technology, Cambridge, Massachusetts 02139, United States;* orcid.org/0000-0002-5988-0677; Email: joppenhe@mit.edu

Mircea Dincă − *Department of Chemistry and Department of Chemical Engineering, Massachusetts Institute of Technology, Cambridge, Massachusetts 02139, United States;* orcid.org/0000-0002-1262-1264; Email: mdinca@mit.edu

Authors

Karla Ravin − *Department of Chemistry, Massachusetts Institute of Technology, Cambridge, Massachusetts 02139, United States*

Patrick Sarver − *Department of Chemistry, Massachusetts Institute of Technology, Cambridge, Massachusetts 02139, United States;* orcid.org/0000-0001-7227-8966

Bhavish Dinakar − *Department of Chemical Engineering, Massachusetts Institute of Technology, Cambridge, Massachusetts 02139, United States;* orcid.org/0000-0002-7611-101X

Lukáš Palatinus − *Institute of Physics of the Czech Academy of Sciences, 18200 Prague, Czechia;* orcid.org/0000-0002-8987-8164

Peter Müller − *Department of Chemistry, Massachusetts Institute of Technology, Cambridge, Massachusetts 02139, United States;* orcid.org/0000-0001-6530-3852

Complete contact information is available at: https://pubs.acs.org/10.1021/jacs.5c01062

Author Contributions

This manuscript was written through contributions of all authors. All authors have given approval to the final version of the manuscript.

Funding

This research was supported by the National Science Foundation (DMR-2105495). We would like to acknowledge the MIT-Czech Republic Seed Fund program at the MIT International Science and Technology Initiatives (MISTI) for travel support. L.P. acknowledges the support by the Czech Science Foundation, project number 21-05926X. L.P. is supported by the project Terafit and CzechNanoLab Research Infrastructure, both supported by MEYS CR (project numbers CZ.02.01.01/00/22_008/0004594 and LM2023051). P.J.S. thanks the National Institute of General Medical Sciences of the National Institutes of Health for postdoctoral fellowship support (F32 GM147937).

Notes

The authors declare no competing financial interest.

ACKNOWLEDGMENTS

We would like to thank Professor Davide Proserpio and Professor Dalal Alezi for invaluable discussions about the topology of the framework.

REFERENCES

(1) An, Y.; Lv, X.; Jiang, W.; Wang, L.; Shi, Y.; Hang, X.; Pang, H. The Stability of MOFs in Aqueous Solutions—Research Progress and Prospects. *Green Chemical Engineering* **2024**, *5* (2), 187−204.

(2) Chae, H. K.; Siberio-Pérez, D. Y.; Kim, J.; Go, Y.; Eddaoudi, M.; Matzger, A. J.; O'Keeffe, M.; Yaghi, O. M. A Route to High Surface Area, Porosity and Inclusion of Large Molecules in Crystals. *Nature* **2004**, *427* (6974), 523−527.

(3) Bezrukov, A. A.; O'Hearn, D. J.; Gascón-Pérez, V.; Darwish, S.; Kumar, A.; Sanda, S.; Kumar, N.; Francis, K.; Zaworotko, M. J. Metal-Organic Frameworks as Regeneration Optimized Sorbents for Atmospheric Water Harvesting. *Cell Reports Physical Science* **2023**, *4* (2), No. 101252.

(4) Logan, M. W.; Langevin, S.; Xia, Z. Reversible Atmospheric Water Harvesting Using Metal-Organic Frameworks. *Sci. Rep* **2020**, *10* (1), 1492.

(5) Rieth, A. J.; Wright, A. M.; Dincă, M. Kinetic Stability of Metal−Organic Frameworks for Corrosive and Coordinating Gas Capture. *Nat. Rev. Mater.* **2019**, *4* (11), 708−725.

(6) Alezi, D.; Oppenheim, J. J.; Sarver, P. J.; Iliescu, A.; Dinakar, B.; Dincă, M. Tunable Low−Relative Humidity and High−Capacity Water Adsorption in a Bibenzotriazole Metal−Organic Framework. *J. Am. Chem. Soc.* **2023**, *145* (46), 25233−25241.

(7) Rieth, A. J.; Wright, A. M.; Skorupskii, G.; Mancuso, J. L.; Hendon, C. H.; Dincă, M. Record-Setting Sorbents for Reversible Water Uptake by Systematic Anion Exchanges in Metal−Organic Frameworks. *J. Am. Chem. Soc.* **2019**, *141* (35), 13858−13866.

(8) Bagi, S.; Wright, A. M.; Oppenheim, J.; Dincă, M.; Román-Leshkov, Y. Accelerated Synthesis of a Ni2Cl2(BTDD) Metal−Organic Framework in a Continuous Flow Reactor for Atmospheric Water Capture. *ACS Sustainable Chem. Eng.* **2021**, *9* (11), 3996−4003.

(9) Wright, A. M.; Rieth, A. J.; Yang, S.; Wang, E. N.; Dincă, M. Precise Control of Pore Hydrophilicity Enabled by Post-Synthetic

Cation Exchange in Metal−Organic Frameworks. *Chem. Sci.* **2018**, *9* (15), 3856−3859.
(10) Rieth, A. J.; Yang, S.; Wang, E. N.; Dincă, M. Record Atmospheric Fresh Water Capture and Heat Transfer with a Material Operating at the Water Uptake Reversibility Limit. *ACS Cent. Sci.* **2017**, *3* (6), 668−672.
(11) Biswas, S.; Grzywa, M.; Nayek, H. P.; Dehnen, S.; Senkovska, I.; Kaskel, S.; Volkmer, D. A Cubic Coordination Framework Constructed from Benzobistriazolate Ligands and Zinc Ions Having Selective Gas Sorption Properties. *Dalton Trans.* **2009**, *33*, 6487−6495.
(12) Oppenheim, J. J.; Ho, C.-H.; Alezi, D.; Andrews, J. L.; Chen, T.; Dinakar, B.; Paesani, F.; Dincă, M. Cooperative Interactions with Water Drive Hysteresis in a Hydrophilic Metal−Organic Framework. *Chem. Mater.* **2024**, *36* (7), 3395−3404.
(13) Safy, M. E. A.; Amin, M.; Haikal, R. R.; Elshazly, B.; Wang, J.; Wang, Y.; Wöll, C.; Alkordi, M. H. Probing the Water Stability Limits and Degradation Pathways of Metal−Organic Frameworks. *Chem.−A Eur. J.* **2020**, *26* (31), 7109−7117.
(14) Kim, H. K.; Jung, J.-Y.; Kang, G.; Baik, M.-H.; Choi, E.-Y. Installing a Molecular Truss Beam Stabilizes MOF Structures. *npj Comput. Mater.* **2022**, *8* (1), 1−9.
(15) Denysenko, D.; Grzywa, M.; Tonigold, M.; Streppel, B.; Krkljus, I.; Hirscher, M.; Mugnaioli, E.; Kolb, U.; Hanss, J.; Volkmer, D. Elucidating Gating Effects for Hydrogen Sorption in MFU-4-Type Triazolate-Based Metal−Organic Frameworks Featuring Different Pore Sizes. *Chem.−A Eur. J.* **2011**, *17* (6), 1837−1848.
(16) Furukawa, H.; Gándara, F.; Zhang, Y.-B.; Jiang, J.; Queen, W. L.; Hudson, M. R.; Yaghi, O. M. Water Adsorption in Porous Metal−Organic Frameworks and Related Materials. *J. Am. Chem. Soc.* **2014**, *136* (11), 4369−4381.
(17) Liu, X.; Wang, X.; Kapteijn, F. Water and Metal−Organic Frameworks: From Interaction toward Utilization. *Chem. Rev.* **2020**, *120* (16), 8303−8377.
(18) Schmieder, P.; Denysenko, D.; Grzywa, M.; Baumgärtner, B.; Senkovska, I.; Kaskel, S.; Sastre, G.; van Wüllen, L.; Volkmer, D. CFA-1: The First Chiral Metal−Organic Framework Containing Kuratowski-Type Secondary Building Units. *Dalton Trans.* **2013**, *42* (30), 10786−10797.
(19) Liu, Q.; Hoefer, N.; Berkbigler, G.; Cui, Z.; Liu, T.; Co, A. C.; McComb, D. W.; Wade, C. R. Strong CO2 Chemisorption in a Metal−Organic Framework with Proximate Zn−OH Groups. *Inorg. Chem.* **2022**, *61* (46), 18710−18718.
(20) Schmieder, P.; Grzywa, M.; Denysenko, D.; Hambach, M.; Volkmer, D. CFA-7: An Interpenetrated Metal−Organic Framework of the MFU-4 Family. *Dalton Trans.* **2015**, *44* (29), 13060−13070.
(21) Röß-Ohlenroth, R.; Kraft, M.; Bunzen, H.; Volkmer, D. Inhibition, Binding of Organometallics, and Thermally Induced CO Release in an MFU-4-Type Metal−Organic Framework Scaffold with Open Bidentate Bibenzimidazole Coordination Sites. *Inorg. Chem.* **2022**, *61* (41), 16380−16389.

https://doi.org/10.1021/jacs.5c01062
J. Am. Chem. Soc. XXXX, XXX, XXX−XXX